

SLAC-PUB-9624
January 2003

COMBINING ELECTRIC AND SAIL PROPULSION FOR INTERPLANETARY SAMPLE RETURN*

Robert J. Noble

Stanford Linear Accelerator Center, Stanford University
2575 Sand Hill Road, Menlo Park, California 94025 USA

Abstract

Fast sample return from the outer Solar System would open an entirely new avenue for space science, but the vast distances make this a daunting task. The achievable transit velocity and the need for extra propellant on the return trip limit the feasibility of returning extraterrestrial samples to Earth. To keep the mission duration short enough to be of interest, sample return from objects farther out in the Solar System requires increasingly higher velocities. High specific impulse, electric propulsion reduces the propellant required for the outbound and return trips, but decelerating the spacecraft at the inner Solar System from high velocity still involves a long, inward spiral trajectory. The use of solar sails to *rapidly decelerate* incoming sample capsules and eliminate propellant is explored in this paper. The sail is essentially a “solar parachute” used for braking at the *end* of the interplanetary return flight, permitting a higher transit speed and truncating the deceleration spiral. In this application the sail is relatively small and manageable since only the sample capsule and its sail are decelerated. A comparison is made between using all-electric propulsion versus combining electric propulsive acceleration with sail deceleration for sample return from the distances of Saturn, Uranus, and Pluto. Solar-sail braking dramatically reduces the return flight time by *one-third or more* compared to using electric rocket deceleration. To elucidate the technology requirements, wide ranges for both the loaded sail density and electric propulsion specific mass are considered in this initial parametric study.

Presented at the 28th International Electric Propulsion Conf., 17-21 March 2003, Toulouse, France.

* Work supported by Department of Energy contract DE-AC03-76SF00515.

1. Introduction

The primary methods for investigating extraterrestrial objects are remote sensing, either from Earth or a spacecraft, in-situ analysis, and sample return. Remote sensing can provide an overview of an object but at the expense of missing local details. In-situ analysis can explore these details, but the science is limited by the number of experiments that can be carried on-board a robotic lander, as was the case with the Viking missions to Mars in search of life. Because of the wide array of tests that can be performed on a sample in a terrestrial or space-station laboratory, sample return would often be preferred if it could be done in a timely fashion and at an acceptable cost. The desire to answer basic questions regarding the origin of the Solar System will motivate robotic sample return missions to increasingly distant objects.

Propulsion and power have always limited the feasibility of sample return missions. This type of mission inherently involves twice the interplanetary velocity change of a one-way rendezvous mission. Because the initial to final mass ratio of a rocket increases exponentially with velocity change, propellant masses can become unrealistic for velocity changes greater than a few times the rocket's exhaust velocity. More distant targets demand ever-higher spacecraft velocities to keep the mission duration short enough to be of scientific interest. Pluto and its moon Charon, at a distance of over 30 Astronomical Units ($1 \text{ AU} = 1.496 \times 10^8$ kilometers is the Earth-Sun separation), have yet to be visited by any robotic craft because of the tremendous cost of chemically launching even a modestly rapid fly-by mission. Fast sample return from locations such as this would open an entirely new avenue for space science, but the vast distances make this a daunting task.

Electric propulsion (EP), which expels ions at high velocity to attain a large momentum transfer with reduced propellant consumption, has long been recognized as an efficient solution for high velocity space missions. Solar electric propulsion has been successfully demonstrated on the Deep Space One mission [1]. The use of electric propulsion for fast robotic missions far from the Sun is the next logical step. Without adequate sunlight for solar electric power in the outer Solar System, the only near-term heat sources available to generate electricity are nuclear. Anticipating new developments in space electric generators and long-life ion engines, various trade studies have been performed in recent years for nuclear electric propulsion (NEP) [2-4] and radioisotope electric propulsion (REP) [5-8] applied to robotic science missions in the outer Solar System. NEP uses a nuclear reactor as a heat source to generate electricity, and REP uses decay heat from a radioisotope inventory. Augmenting EP with an initial impulse of a few kilometers per second with a disposable chemical rocket at Earth escape further shortens the rendezvous trip times to the outer planets. The rendezvous trip time to Pluto can be reduced to about ten years in this way.

Given that relatively short trip times will be possible from Earth to the outer Solar System in the next decade, it is appropriate to visit the subject of robotic sample return from distant objects. The generic scheme for a deep-space sample return mission involves a parent craft flying out from Earth to rendezvous with a target body. This craft or a lander descends and collects a sample. The sample is provided to a special, dedicated return vehicle, which has its own propellant and optimized electric propulsion unit. This small sample-return vehicle is the only object to fly back to Earth, while the parent craft continues an extended science mission at the body or moves on to another target. With the Sun's gravity helping the acceleration of the small return vehicle, the electric rocket quickly builds up a high return velocity. Approaching the inner Solar System, the electric rocket with its extraterrestrial sample decelerates in a long, inward spiral trajectory (essentially the reverse of an escape spiral), as shown in the solid curve of Figure 1, until it reaches the Earth's sphere of influence, where it can be retrieved. Unfortunately, several years of the sample-return mission can be spent spiraling inward within just a few AU of the Sun. Typically about *one-third* of the in-bound trip time is spent in this low-thrust deceleration phase approaching Earth.

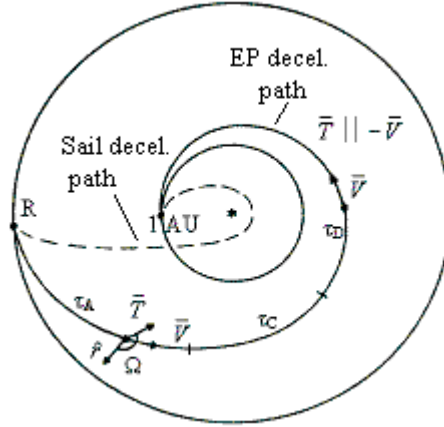


Figure 1. Spiral return trajectory for a low-thrust EP rocket showing the acceleration, coast, and deceleration phases (solid), and an alternate fast-return trajectory possible with solar sail deceleration (dashed). \bar{T} is the thrust vector, \bar{V} is the velocity vector, and \hat{r} is the solar radial unit vector.

In this paper, a new hybrid propulsion scheme is explored for fast sample return from the outer Solar System. A sample return mission involves several complicated steps to reach a target and obtain a sample, *but only the interplanetary return phase of the mission is addressed here*. Our method exploits the natural strengths of two different propulsion technologies: electric and solar sail. Acceleration of the sample-return vehicle toward the Sun for the inbound trip from deep space is done with a disposable, electric propulsion stage. Upon approaching the inner Solar System this EP stage is *jettisoned*, and the sample capsule deploys a solar sail for rapid deceleration and matching to the Earth's orbit. A solar sail operates on the principle of momentum transfer by incident and reflected sunlight [9]. Sail acceleration is inversely proportional to both the sail mass per unit area and the square of the distance to the Sun. Solar sails have often been suggested in the past for enabling high-velocity, outbound missions. In this paper we introduce the sail as a “solar parachute” for braking at the *end* of the interplanetary return flight. As illustrated by the dashed curve in Figure 1, this solution permits the inbound trajectory to be at a much higher velocity and more directly radial than with low-thrust electric deceleration. Propellant is eliminated, the deceleration spiral is truncated, and the return flight duration can be reduced by *one-third or more* with sail deceleration as compared to using electric rocket deceleration. Importantly, *the sail areas are relatively small and manageable in this application* since only the sample capsule and its sail are decelerated (e.g., for a total sailcraft mass of 50 kg, including sample, and a sailcraft loading of 10 grams/meter², a square sail is only 70 meters on a side).

In this initial parametric study, return flight times for missions using all-electric propulsion (the benchmark) and electric propulsion combined with sail deceleration are compared. To elucidate the technology requirements, wide ranges for the two critical figures of merit, EP specific mass (rocket powerplant mass per unit thrust power) and sail loading (total sailcraft mass divided by sail area), are considered. Many results for sample-return trajectories from Pluto-Charon are presented because of the scientific interest in that unexplored system. Using the hybrid electric-sail technique, the return times from Pluto are in the range of 8.6 to 10 years for sail loadings of 6 to 8 grams/meter² and an EP powerplant specific mass of 100 kg/kW. Special results are also presented for return trajectories from the distances of Uranus and Saturn. The satellites of both these worlds certainly hold important clues about the early Solar System. We find that an all-electric propulsion system with $\alpha = 100$ kg/kW gives return flight-times from Saturn and Uranus of 4.5 and 8.3 years, respectively. But combining EP acceleration with solar-sail deceleration dramatically reduces the return times from

these planets to only 3.2 and 5.6 years, respectively. With the introduction of solar sail deceleration, the outer planet regions can be opened to fast and repeated sample-return missions.

2. Electric and Solar Sail Propulsion

Significant progress has been made in recent years in both electric propulsion and solar sail technologies. A wide range of proposed scientific and observational missions with special trajectory or velocity requirements continues to motivate this work. The availability of these propulsion technologies will lead to new hybrid propulsion schemes that will enable missions previously thought to be unachievable. A broad literature exists covering the state-of-the-art and expectations for near-term improvements in space electric power generation [10, 11], electric propulsion [12, 13, 14], and solar sail technologies [9, 15]. Our purpose is not to review these technologies in detail but only to introduce the relevant figures of merit for the trajectory studies to follow.

Primary electric propulsion is only feasible if an efficient space electric power source and long-life thrusters exist. The availability of electric power also impacts the scientific program since data collection at the source and the data transmission rate to Earth are proportional to available power. For rocket propulsion, the relevant figure of merit is the powerplant specific mass α , which is the total mass of the electric generator plus rocket engines per unit thrust power. In free space, the maximum velocity change scales like $(\tau / \alpha)^{1/2}$, where τ is the thrust time. Within about 3 AU of the Sun, solar cells provide enough electric power per mass to be useful for primary electric propulsion, as demonstrated on the Deep Space One mission. For EP far from the Sun, only nuclear heat sources are available for the conceivable future. Nuclear electric propulsion (NEP) generally refers to any ion or plasma propulsion system powered by electricity generated with a nuclear reactor heat source. Due to the requirements of a critical nuclear mass and a large reactor vessel mass with containment, moderator, cooling and control systems, these generators have a favorable economy of scale for electric powers above tens of kilowatts. Powerplant specific masses of proposed NEP systems have been estimated in the range of 20 to 50 kg/kW of thrust power. They are appropriate for 1000 kg-class and larger robotic craft, which require high power thrusters (10 kW and higher) simply due to their bulk.

Radioisotope electric propulsion (REP) refers to systems in which the heat source for generating electricity is an onboard radioisotope inventory. The thermal power per unit mass of active isotope is determined only by the decay energy and nuclear half-life. Plutonium-238 has been commonly used because of its convenient 86-year half-life and its availability as a by-product of weapons production. New Pu-238 isotope has a mass to thermal power ratio of about 1 kilogram per kilowatt of heat. Hardware mass is actually dominated by the electric generator in radioisotope systems, not a nuclear reactor vessel and cooling components. The standard semiconductor thermoelectric cells based on the Seebeck effect have been used on all the deep-space robotic craft to date. Their thermal to electric efficiency is only about 6 percent, and consequently they have not been of interest for propulsion applications. Several other technologies for generating electricity from radioisotope heat have been explored over the years. These include, thermo-photovoltaic cells, alkali-metal thermal-electric cells, and Stirling-cycle, free-piston alternators. Due to the modularity of these generators, REP scales gracefully to lower powers and is well suited to small robotic probes with masses of tens to hundreds of kilograms and propulsive power requirements of order kilowatts or less. Powerplant specific masses of proposed near-term REP systems are estimated in the range of 100 to 200 kg/kW, although lower values may be possible with development. REP is ideal for the sample-return leg of a deep-space robotic mission since the return vehicle is small (e.g. < 100 kg total mass), the radioisotope power system has few or no moving parts with concomitant low risk of start-up problems after years of storage, and the radioisotope provides a natural heat source for the dormant craft on the outbound journey.

All conventional rockets, which take along propellant for momentum transfer, suffer from an exponentially increasing initial mass for higher rocket velocities. Placing the propellant off the

vehicle removes a basic constraint of the rocket equation. A solar sail operates on the principle of momentum transfer by incident and reflected sunlight. The product of solar radiation pressure multiplied by the projected sail area in the direction toward the Sun gives the incident radiation force on a sail. A number of parameters including the sail's pitch angle, reflection coefficient and thermal emissivity determine the net radial and angular force components experienced. The Sun's radiation pressure is $P_s = 4.51 \times 10^{-6}$ Newton/meter² at 1 AU and varies inversely with the square of the distance. Sail acceleration is inversely proportional to both the sail mass per unit area and the square of the distance to the Sun. Because a sailcraft has many components that contribute to its mass besides the sail, the basic figure of merit for propulsion considerations is the total vehicle mass divided by sail area, which is called the effective sail areal density, σ_{eff} , or simply the "sail loading".

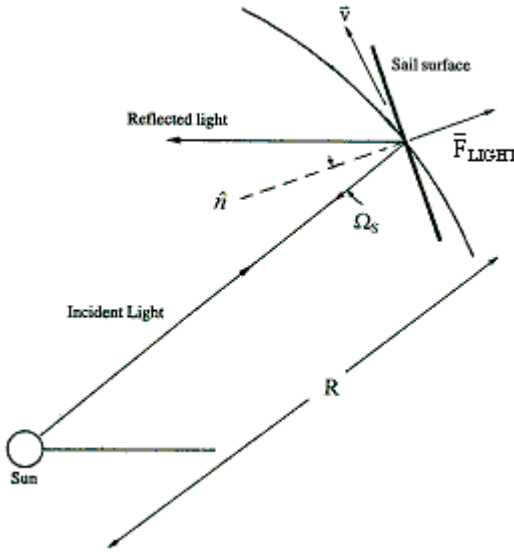


Figure 2. Radiation force on an ideal solar sail is normal to the sail surface.

For an initial feasibility study, the ideal sail approximation is completely adequate and is used in this paper. An ideal sail is flat (no billowing under load) and is a specular reflector (no diffuse reflection) with a reflection coefficient of one (no absorption or transmission) over the entire solar spectrum. In this case the net acceleration from the incident and reflected light is directed normal to the sail surface (Figure 2), and the magnitude is given by $a_n = 2(P_s/\sigma_{\text{eff}})(R_e/R)^2 \cos^2\Omega_s$. Here the sail pitch angle Ω_s is the angle between the sail normal and the solar radial vector, $R_e = 1$ AU, R is the sailcraft's distance from the Sun, $\sigma_{\text{eff}} = (\sigma_s A + m_p)/A$, A is the sail area, σ_s is the mass of the sail plus supporting structure divided by the sail area, and m_p is the payload mass. Because real sails are highly reflecting (typically better than 90 percent) and nearly specular (typically better than 94 percent), this is a good approximation as long as the pitch angle is less than about 45 degrees. Beyond this angle, the difference between the true direction of the force vector and the sail normal exceeds 5 degrees, producing a noticeable change in calculated trajectories [9]. Such corrections are only important for detailed mission and navigation calculations. In our sail deceleration calculations however, sail pitch angles are found to be typically less than 25 degrees. Neglecting the pointing correction then, the main effect that must be included is the reflection coefficient, r , being less than unity, which reduces the sail acceleration by the factor $(1+r)/2$. The leading dynamic effect is to reduce sail performance by increasing the effective sail loading value in the equations of motion. This means that in all of our plots, the reader may take σ_{eff} to mean $2\sigma_{\text{eff}}/(1+r)$ when r is close one.

Next to fabricating lightweight, highly reflecting sails, the most challenging task in reducing the sailcraft loading is to decrease the mass of command and controls, bus work, thermal

management, power management and distribution, and ancillary flight equipment. Many of these involve established technology items that are flight-proven but heavy [15]. For large sails with masses of hundreds of kilograms, these items can be a small fraction of the total mass, but in a small sailcraft for sample-return missions, they can dominate the mass budget and make the sail loading so high that the acceleration advantage of sail propulsion is completely lost. The successful application of sail propulsion for small sciencecraft will depend on developing advanced microelectronics and lightweight spacecraft bus and controls.

3. Sample Return with All-Electric Propulsion

Once primary electric propulsion is available for deep-space rendezvous missions, it will be natural to extend its use for robotic sample return to Earth. This application naturally does not introduce any new risk to a mission that already uses EP for the outbound voyage. Some authors have considered using EP for sample return from near-Earth asteroids and incoming comets. Electric propulsion is clearly the benchmark to compare other concepts for sample return from the outer Solar System. This section presents interplanetary trajectory studies for sample return from the environs of Pluto, Uranus, and Saturn using all electric propulsion. These results form the basis for the comparison of EP with solar sail deceleration in the next section.

To simplify the analysis, only constant exhaust velocity and constant thrust ion engines are considered for these calculations. The use of ion engines that have variable thrust and specific impulse are expected to yield somewhat improved flight times, typically at the level of 10 percent. The generic constant thrust trajectory was shown in Figure 1. All planets are approximated to lie in the ecliptic plane, which although usually a poor model for Pluto's orbit, is perfectly adequate for all flight time estimates. The sheer distances to the outer planets basically determine the return times, and plane changes introduce minor corrections.

For interplanetary rocket transfer, four quantities must be specified to determine a final orbit relative to an initial orbit in the same plane. Typically these are the semimajor axis, the eccentricity, the argument of perihelion, and the epoch of perihelion. Four mission parameters must then be selected to match the rocket's final trajectory with the desired target orbit. The departure date from the initial body provides one parameter to insure that the rocket meets the destination orbit at a particular time. The acceleration thrust time, the ion thrust angle (relative to the Sun's radial vector, for example), and the deceleration thrust time can be used as the other three parameters. The deceleration thrust angle is aligned exactly opposite to the velocity vector during the braking maneuver and is not a free parameter in our study. With these choices, the coast time (the period of no thrusting between the acceleration and deceleration phases) is the only free parameter in our thrust program to minimize the flight time. This program fully describes the trajectory matching constraints, but not the rocket configuration, i.e. the choice of mass fraction for the rocket's powerplant and propellant.

In an optimization to maximize the payload delivered in the shortest flight time, all trajectory and rocket parameters are varied simultaneously. In Reference 5, it was found that for constant-thrust rockets which spend a significant fraction of time in the weak gravitational fields beyond a few AU from the Sun, the rocket configuration that maximized the payload mass was roughly that for a rocket in field-free space, nearly independent of the exact trajectory. In this case, the ratio K of the powerplant mass to propellant mass is given approximately by the empirical formula $K_{opt} = 0.26(1+2 \ln(1+3 M_L/M_O))$, where M_L is the desired maximum payload mass, and M_O is the initial rocket mass (sum of payload, powerplant and propellant). This simplified rocket configuration is adopted for all calculations in this paper. The effective propellant velocity $v'_p = \eta_m v_p = K v'_c$, where $v'_c = (2\tau \eta_t/\alpha)^{1/2}$ is the powerplant's characteristic velocity, η_t is the rocket's total efficiency, η_m is the thruster's mass utilization efficiency, and v_p is the actual exhaust velocity. Note that effective powerplant specific mass α/η_t is the relevant figure of merit for the propulsion system.

Figure 3 shows the return flight time to the Earth’s 1 AU circular orbit from the distances of Saturn (9.5 AU), Uranus (19.3 AU), and Pluto (34.2 AU in 2020) as a function of the EP powerplant effective specific mass α/η_t when the payload fraction of the returning electric rocket is 0.125, and $K_{opt} = 0.43$. These are the minimum flight times for constant-thrust trajectories illustrated in Figure 1 in which the coast period is the only free parameter. Table 1 lists the ratio of the optimal coast duration to the return flight time for the missions in Figure 3. Roughly a third of the flight is spent in the coast phase and two-thirds in the powered phase. The scaling of flight time with the planet’s distance from the Sun is approximately $R^{0.8}$, which is to be compared to the familiar Hohmann transfer time which scales as $R^{3/2}$. Note in Figure 3 that the flight time scales roughly as $(\alpha/\eta_t)^{0.5}$, which not surprisingly is about the same scaling found in Ref. 5 for *outbound* rendezvous trajectories starting at 1 AU. Return times from beyond Saturn are very long unless the powerplant specific mass α/η_t is 100 kg/kW or less. High-performance propulsion technologies must be developed before significantly shorter trips are possible. An important reason for the long return times is the large fraction of time spent by the EP rocket decelerating at the *inner* Solar System, as illustrated in Table 2. Roughly *one-third* of the return time is spent in the final deceleration spiral approaching the Earth.

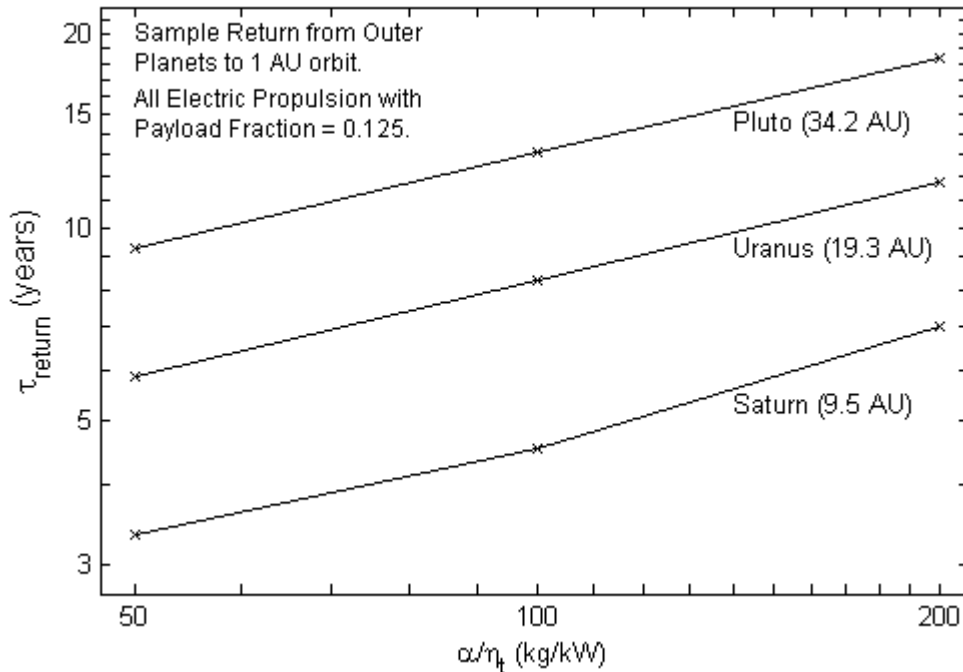


Figure 3. Sample return time from the outer planets to a 1 AU Earth orbit as a function of powerplant specific mass using all-electric propulsion.

Table 1: Fraction of flight time spent in optimal coast phase as a function of powerplant specific mass for all-EP sample return missions with a payload fraction of 0.125.

$\tau_{coast} / \tau_{return}$	Saturn	Uranus	Pluto
$\alpha/\eta_t = 50$ kg/kW	0.42	0.39	0.40
$\alpha/\eta_t = 100$ kg/kW	0.40	0.38	0.36
$\alpha/\eta_t = 200$ kg/kW	0.31	0.30	0.34

Table 2: Fraction of flight time spent in the deceleration phase as a function of powerplant specific mass for all-EP sample return missions with a payload fraction of 0.125.

$\tau_{\text{decel}} / \tau_{\text{return}}$	Saturn	Uranus	Pluto
$\alpha/\eta_t = 50 \text{ kg/kW}$	0.23	0.25	0.24
$\alpha/\eta_t = 100 \text{ kg/kW}$	0.30	0.30	0.30
$\alpha/\eta_t = 200 \text{ kg/kW}$	0.42	0.39	0.34

To give some insight into the trade-off of flight time versus increased payload mass fraction of the EP return vehicle, sample return from Pluto was compared for payload fractions of 0.25 ($K_{\text{opt}} = 0.54$) and 0.125 ($K_{\text{opt}} = 0.43$). The return times versus powerplant specific mass are illustrated in Figure 4, with an increase of about 30% in flight time resulting for the larger payload. There is a significant increase in scientific return for only a slightly greater flight time.

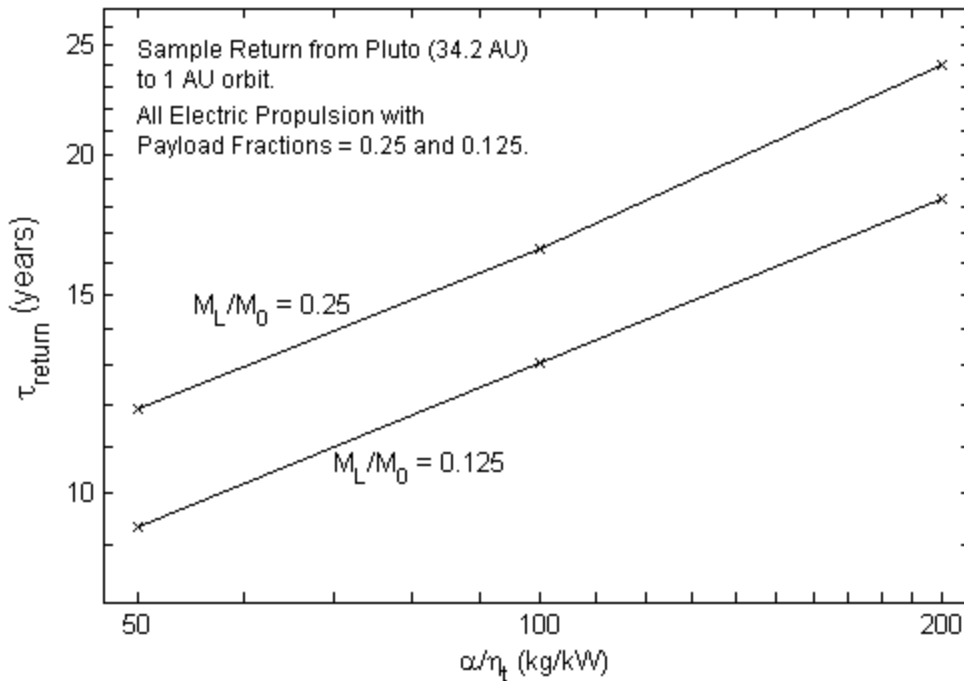


Figure 4. Sample return time from Pluto (departure in 2020) to a 1 AU Earth orbit as a function of EP powerplant specific mass for different payload mass fractions (M_L/M_0) of the return rocket.

4. Fast Sample Return with Solar Sail Deceleration

This section presents trajectory calculations for sample return from the same outer planet regions as in the previous section using solar sail deceleration in place of electric propulsion at the end of the mission. Comparing the performance of the all-electric propulsion technique to the hybrid EP-sail technique is complicated somewhat by the possible choices of payload fraction. The sailcraft with its sample capsule represents the “payload” for the hybrid rocket, with the EP rocket being jettisoned just prior to sail deployment. On the other hand, for the all-EP rocket, the payload is the sample capsule alone. Hence a full comparison of these two propulsion schemes would require the introduction of a new parameter, the mass ratio of the empty sailcraft to sample capsule, which would be varied in the study. We note however that there is a natural choice for this mass ratio, which makes very efficient use of a sail for *sample return missions*, namely unity. As pointed out in Section

2, the loaded sailcraft density σ_{eff} determines the craft's acceleration capability. If the payload mass dominates the sailcraft mass budget, then σ_{eff} is much greater than that of the raw sail material, and the acceleration advantage of a light sail material is lost. If instead the sail mass dominates the mass budget, then mission resources are being used to transport primarily sail material around the Solar System and not returned samples, negating the whole point of the technique. As a reasonable compromise, we adopt the mass ratio of the empty sailcraft to the sample capsule (with sample) as unity. Then to compare an EP-sail hybrid rocket's performance with the all-EP rocket in Section 3 with its 0.125 payload fraction, we will use a payload fraction of 0.25 in the hybrid rocket: the sample capsule and empty sailcraft each separately comprises a mass fraction of 0.125 of the full return craft when it departs the target for the inbound trip. In this comparison, an equal capsule mass fraction (0.125) is returned to Earth by both the hybrid rocket and the EP rocket in Section 3.

Just as for the all-EP case, three mission parameters must be specified to match the return vehicle's trajectory to the desired final orbit in the inner Solar System, with the departure date setting the correct arrival time. The three parameters we adopt are the ion acceleration thrust time, the ion thrust angle (relative to the Sun's radial vector again), and the sail deceleration thrust time. The sail pitch angle Ω_s (see Figure 2) is set to be a constant during the deceleration phase. For any autonomous sciencecraft this represents a very robust navigation program for the on-board computer with only minor sail reorientations required for in-flight course corrections. The coast period and the sail pitch angle can in fact be used as free parameters in a trajectory study to minimize the flight time. We found that flight time is insensitive to coast period since the sail is ineffective beyond several AU and deploying it early does not change the dynamics much. Optimal sail pitch angles are typically in the narrow range of 20 to 25 degrees, except for sails below about 4 grams/m² where optimal sail angles drop to the range of 2 to 20 degrees.

The deceleration path with sail braking from the outer Solar System can be much more direct and faster than with EP braking since the sail's ability to take out both radial velocity and angular momentum increases rapidly as the Sun is approached. Indeed the fastest return paths involve making a close encounter with the Sun where most deceleration by the sail occurs near perihelion, as illustrated in Figure 1. Great advantage is obtained if this perihelion point is in fact on an orbit with a 1 AU aphelion, for then the sailcraft can *automatically rendezvous with Earth* on the outward, free-return Hohmann ellipse, using the sail only for minor course corrections. Two particular transfer orbits are preferred: the 2:1 Earth resonance orbit with perihelion 0.26 AU and the 3:2 resonance orbit with perihelion 0.53 AU. The 2:1 orbit has a period of 1/2 year, making two solar revolutions for every one by the Earth, while the 3:2 orbit has a period of 2/3 year. These orbits are preferred since if for some reason the sample capsule is not successfully intercepted at Earth on the first pass, it will periodically return to the Earth's neighborhood every 1 or 2 years, respectively, along these "safe orbits" for subsequent retrieval. The final Earth rendezvous and return of the sample capsule are not studied in this initial paper since many viable options are available for analysis. For example, the sailcraft could make a Lagrange point or high Earth-orbit rendezvous, or a direct atmospheric re-entry as planned for the Stardust comet sample return mission.

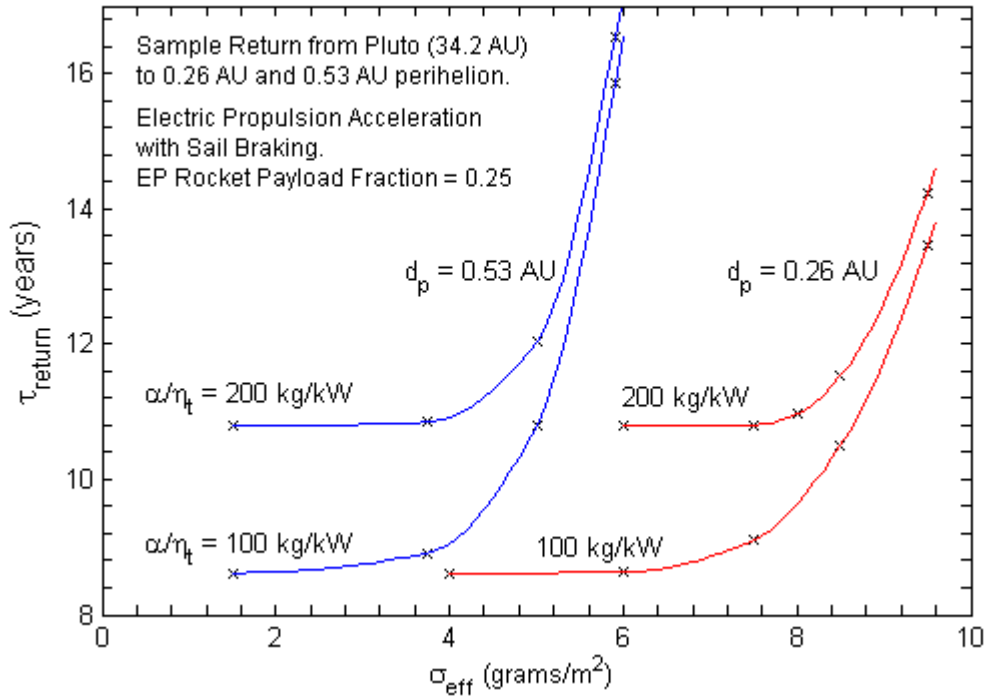


Figure 5. Sample return time from Pluto (departure in 2020) with sail deceleration to 0.26 AU and 0.53 AU perihelion points versus sailcraft loading. Results for different powerplant specific masses of the EP return rocket are illustrated.

Figure 5 illustrates the sample return time from Pluto (departure in the year 2020) with sail deceleration to the “safe-orbits” having perihelions of 0.26 AU and 0.53 AU versus the effective sailcraft loading (total sailcraft mass per sail area). Because of the four-fold increase in solar intensity between 0.53 and 0.26 AU, the closer perihelion enables the use of much heavier sails for the same flight time. From these perihelion points, Earth is then reached 3 or 4 months later, respectively, on the outward Hohmann ellipse. Results are shown for powerplant specific masses of $\alpha/\eta_t = 100$ and 200 kg/kW for the EP rocket that accelerates the sample return vehicle toward Earth. This is the expected α/η_t range for future REP powerplants, which are very attractive for the return of 1 to 10 kilogram-size samples. Naturally a lower α/η_t means a higher return velocity and a shorter trip time. Lower density sails generally result in shorter trip times because their greater decelerating capability permits the use of higher velocities for the return craft *during more of the inbound trip*. Heavier sails cannot take out as much velocity and in fact must be deployed many AU from the Sun to initiate the braking process early. But the reduced trip time due to lowering the sail density is found to *approach a lower bound* in Figure 5 for the following reason. For lighter sails, the braking time eventually becomes *negligible* compared to the total trip time, while the maximum inbound speed is simply due to the EP rocket’s impulse plus the gravitational infall toward the Sun. The minimum flight time then is roughly the inbound travel distance divided by this maximum speed and becomes independent of the sail loading. For sample return from Pluto to 0.26 AU perihelion, there is little improvement gained in flight time by pushing the sailcraft loading below 7 grams/m². Comparing Figures 3 and 5, return trip times from Pluto with sail braking are at least one-third shorter than the return times using EP rocket deceleration for the same α/η_t and the same mass fraction for the sample capsule.

The advantage of sail braking is equally dramatic for fast sample return from nearer planets like Uranus and Saturn. Figure 6 illustrates sample return times from the outer planets with sail deceleration to a perihelion of 0.26 AU versus sailcraft loading when the EP powerplant specific

mass is 100 kg/kW. The return-time curve for Pluto is identical to Figure 5 and is included for comparison. The scaling of flight time with the planet's distance from the Sun is about $R^{0.8}$. Again, the return-time curves all approach a lower bound as the sail loading is reduced, but for Uranus and Saturn the knees in the curves occur at higher values of σ_{eff} than for Pluto. This is because the sails do not have to take out as much velocity and can thus have a lower decelerating capability, which reduces the demand on sail development for these missions. Fast sample return from Saturn (3.2 yr) and Uranus (5.6 yr) can begin once sailcraft technology achieves loadings of 10 g/m² and 8.5 g/m², respectively.

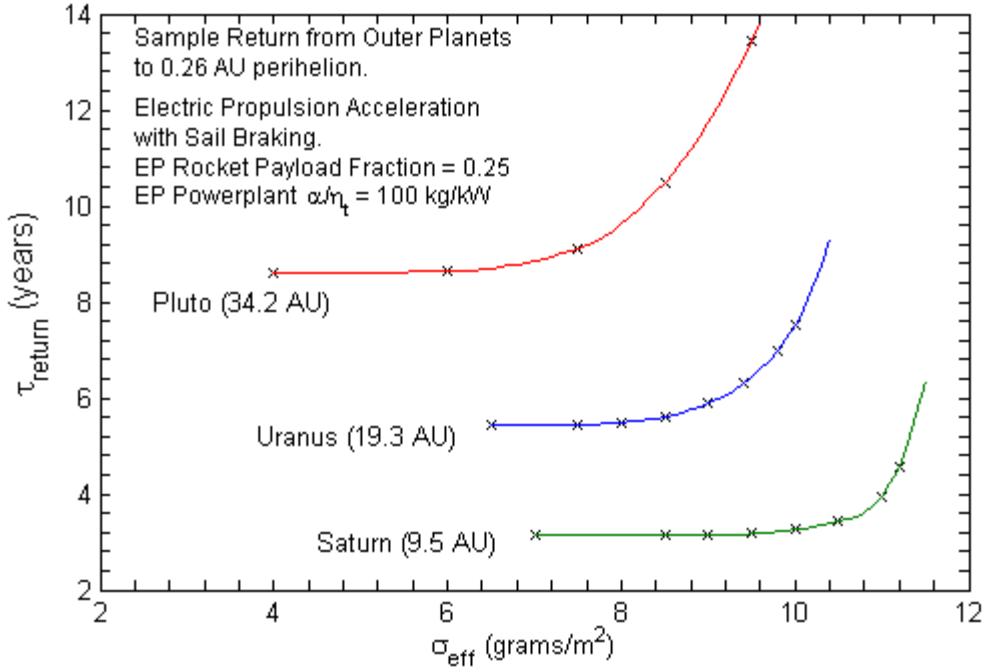


Figure 6. Sample return time from the outer planets with sail deceleration to 0.26 AU perihelion point versus sailcraft loading. The powerplant specific mass of the EP return rocket is 100 kg/kW in these examples.

4. Conclusions

We have compared the use of electric and sail propulsion for decelerating sample return capsules from the outer planets. Because of the slow, inward deceleration spiral that an all-EP rocket must perform, return times from beyond Saturn are very long unless the powerplant specific mass α/η_t is 100 kg/kW or less. Unfortunately return times scale roughly as $(\alpha/\eta_t)^{0.5}$, requiring high-performance propulsion technologies to be developed before significantly shorter trips are possible. The combination of electric propulsive acceleration with solar sail deceleration dramatically shortens the return times by one-third or more compared to using EP deceleration. Sail loadings are in the range of 10 to 7 g/m² for sample return missions from Saturn through Pluto. Importantly, high specific mass EP powerplants of 100 kg/kW or more are completely adequate for the acceleration phase of the return trip, suggesting that exciting sample return missions from the outer Solar System need not await the lengthy development of advanced propulsion systems.

ACKNOWLEDGMENTS

This work was supported by the U.S. Department of Energy under contract DE-AC03-76SF00515. The author wishes to thank Juan Ayon, John Brophy, Charles Garner, Gerhard Kloss, Stephanie Leifer, David Rodgers, Carl Sauer, Jr., Gregg Vane and John L. West at NASA/JPL for discussions and suggestions during the course of this work, Gary Bennett for information on space nuclear power, and Colin McInnes for information on solar sails.

REFERENCES

1. J.E. Polk et al, "Demonstration of the NSTAR Ion Propulsion System on the Deep Space One Mission", IEPC-01-075, 27th Intl. Electric Propulsion Conf., Pasadena, California, October 14-19, 2001.
2. J. Kelley, R. Boain and C. Yen, "Robotic Planetary Science Missions with NEP", Ninth Symposium on Space Nuclear Power Systems, AIP Conference Proc. No. 246, 1992, pp. 78-90.
3. D. Poston, et al, "Fission-Based Electric Propulsion for Interstellar Precursor Mission," in proceedings of *Space Technology and Applications International Forum (STAIF-2000)*, edited by M. El-Genk, AIP Conference Proc. No. 504, New York, 2000, pp. 974-983.
4. R. Lipinski, et al., "NEP for Kuiper Belt Object Rendezvous Mission," in proceedings of *Space Technology and Applications International Forum (STAIF-2000)*, edited by M. El-Genk, AIP Conference Proc. No. 504, New York, 2000, pp. 1192- 1201.
5. R.J. Noble, "Radioisotope Electric Propulsion for Robotic Science Missions to Near-Interstellar Space", J. British Interplanetary Soc., Vol. 49, pp. 322-328, 1996; "Radioisotope Electric Propulsion for Small Robotic Space Probes", J. British Interplanetary Soc., Vol. 49, pp.455-468, 1996.
6. R.J. Noble, "Radioisotope Electric Propulsion of Sciencecraft to the Outer Solar System and Near Interstellar Space", Acta Astronautica, Vol. 44, Nos. 2-4, pp.193-199,1999; An adapted article of the same title also appeared in Nuclear News, pp. 34-40, November 1999 (American Nuclear Society).
7. S. Oleson et al, "Outer Planet Exploration with Advanced Radioisotope Electric Propulsion", IEPC-01-0179, 27th Intl. Electric Propulsion Conf., Pasadena, California, October 14-19, 2001.
8. S. Oleson, et al, "Radioisotope Electric Propulsion for Fast Outer Planetary Orbiters", AIAA 2002-3967, 38th Joint Propulsion Conference, Indianapolis, Indiana, July 7-10, 2002.
9. C. McInnes, *Solar Sailing: Technology, Dynamics and Mission Applications*, Praxis Publ., UK, 1999.
10. G.L. Bennett, R.J. Hemler and A. Schock, "Space Nuclear Power: An Overview", J. Propulsion and Power, Vol. 12, No. 5, pp. 901-910, 1996.
11. G.L. Bennett, "Power for Space Science Missions: The Nuclear Option", presented at the 41st Aerospace Sciences Meeting, AIAA, January 2003, Reno, Nevada.
12. M.J. Patterson, et al, "Ion Propulsion Development Activities at NASA Glenn Research Center", AIAA 2000-3810, 36th Joint Propulsion Conference, Huntsville, Alabama, July 16-19, 2000.
13. N.J. Meckel et al, "High Performance, Low Power Ion Propulsion System Design Concept", IEPC-01-108, 27th Intl. Electric Propulsion Conf., Pasadena, California, October 14-19, 2001.
14. D. Rodgers and J. Brophy, "Ion Propulsion Technology for Fast Missions to Pluto", IEPC-01-176, 27th Intl. Electric Propulsion Conf., Pasadena, California, October 14-19, 2001.
15. J.L. West and B. Derbes, "Solar Sail Vehicle System Design for the Geostorm Warning Mission", AIAA-2000-5326.